Published in final edited form as:

Int J Biochem Cell Biol. 2010 September ; 42(9): 1525–1535.

Interaction of ibogaine with human α3β4-nicotinic acetylcholine receptors in different conformational states

Hugo R. Arias[a,*], **Avraham Rosenberg**[b], **Katarzyna M. Targowska-Duda**[c], **Dominik Feuerbach**[d], **Xiao Juan Yuan**[e], **Krzysztof Jozwiak**[c], **Ruin Moaddel**[b], and **Irving W. Wainer**[b]

[a]Department of Pharmaceutical Sciences, College of Pharmacy, Midwestern University, 19555 N. 59th Ave., Glendale, AZ 85308, USA [b]Gerontology Research Center, National Institute of Aging, NIH, Baltimore, USA [c]Department of Chemistry, Medical University of Lublin, Lublin, Poland [d]Neuroscience Research, Novartis Institutes for Biomedical Research, Basel, Switzerland [e]College of Pharmacy, Western University of Health Sciences, Pomona, CA, USA

Abstract

The interaction of ibogaine and phencyclidine (PCP) with human (h) α3β4-nicotinic acetylcholine receptors (AChRs) in different conformational states was determined by functional and structural approaches including, radioligand binding assays, Ca^{2+} influx detections, and thermodynamic and kinetics measurements. The results established that (a) ibogaine inhibits (±)-epibatidine-induced Ca^{2+} influx in hα3β4 AChRs with ~9-fold higher potency than that for PCP, (b) [^{3}H]ibogaine binds to a single site in the hα3β4 AChR ion channel with relatively high affinity (K_d = 0.46 ± 0.06 μM), and ibogaine inhibits [^{3}H]ibogaine binding to the desensitized hα3β4 AChR with slightly higher affinity compared to the resting AChR. This is explained by a slower dissociation rate from the desensitized ion channel compared to the resting ion channel, and (c) PCP inhibits [^{3}H]ibogaine binding to the hα3β4 AChR, suggesting overlapping sites. The experimental results correlate with the docking simulations suggesting that ibogaine and PCP interact with a binding domain located between the serine (position 6′) and valine/phenylalanine (position 13′) rings. This interaction is mediated mainly by van der Waals contacts, which is in agreement with the observed enthalpic contribution determined by non-linear chromatography. However, the calculated entropic contribution also indicates local conformational changes. Collectively our data suggest that ibogaine and PCP bind to overlapping sites located between the serine and valine/phenylalanine rings, to finally block the AChR ion channel, and in the case of ibogaine, to probably maintain the AChR in the desensitized state for longer time.

Keywords

Nicotinic acetylcholine receptors; Conformational states; Noncompetitive antagonists; Ibogaine; Phencyclidine

[*]Corresponding author. Tel.: +1 623 572 3589; fax: +1 623 572 3550. harias@midwestern.edu (H.R. Arias).

1. Introduction

Drug addiction is a very complex mechanism and involves several brain areas. There are two neuronal pathways that modulate the process of brain reward (reviewed in Maisonneuve and Glick, 2003; Arias, 2009). The main and best known brain reward circuitry, the so-called mesocorticolimbic system, extends from a set of dopamine-producing neurons that originate in the ventral tegmental area (VTA), to dopamine-sensitive cells located in the nucleus accumbens. VTA neurons express several nicotinic acetylcholine receptors (AChRs) including α4β2 and α7 subtypes (reviewed in Mansvelder et al., 2006). The habenulo-interpeduncular cholinergic pathway is considered a second brain reward circuitry where the most important expressed AChR subtype is the α3β4 (Quick et al., 1999; reviewed in Maisonneuve and Glick, 2003). Considering this evidence, possible roles for α4β2, α7, and α3β4 AChRs in the process of drug addiction and consequently as targets for the pharmacological action of anti-addictive drugs have been suggested. AChRs are members of the Cys-loop ligand-gated ion channel superfamily, that includes types A and C γ-aminobutyric acid, type 3 5-hydroxytryptamine (serotonin), and glycine receptors (reviewed in Arias, 2001, 2006; Arias et al., 2006a; Gotti et al., 2006; Albuquerque et al., 2009).

Ibogaine [12-methoxyibogamine or 7-ethyl-6,2,7,8,9,10,12,13-octahydro-2-methoxy-6,9-methano 5H-pyrido(1′,2′:1,2-azepine (4,5-)indole)] is a natural product obtained from the roots of the shrub *Tabernanthe iboga*. This alkaloid decreases drug self-administration in animals (reviewed in Glick et al., 2000; Glick and Maisonneuve, 1998), helps to interrupt drug dependence in humans (reviewed in Vocci and London, 1997), and behaves pharmacologically as a noncompetitive antagonist (NCA) of several AChRs (Arias et al., 2010c; Fryer and Lukas, 1999; Badio et al., 1997; Glick et al., 2002; Pace et al., 2004). In this regard, a better understanding of the interaction of ibogaine with the human (h) α3β4 AChR is crucial to develop novel analogs for safer anti-addictive therapies. The α3β4 AChR is expressed in several brain areas including, medial habenula, interpeduncular nucleus, pineal gland, locus coeruleus, ventral tegmental area, dorsolateral tegmentum, basolateral amygdale, and hippocampus (Glick et al., 2008; reviewed in Gotti et al., 2006). Thus, we want to determine the interaction of ibogaine with hα3β4 AChRs in different conformational states and to compare it to that for phencyclidine (PCP). Phencyclidine is a NCA that has been used for decades to study the structure and function of muscle AChR ion channels (Arias et al., 2003, 2006b, 2010a; Sanghvi et al., 2008; Hamouda et al., 2008; reviewed in Arias et al., 2006a) and inhibits the α3β4 AChR with moderate potency (Fryer and Lukas, 1999). To this end, we used structural and functional approaches including radioligand binding assays using [^{3}H]ibogaine and the PCP analog [piperidyl-3,4-^{3}H(*N*)]-*N*-(1-(2 thienyl)cyclohexyl)-3,4-piperidine ([^{3}H]TCP), Ca^{2+} influx-induced fluorescence detections, thermodynamic and kinetic measurements using non-linear chromatography, and molecular docking studies.

2. Materials and methods

2.1. Materials

[Piperidyl-3,4-^{3}H(*N*)]-(*N*-(1-(2 thienyl)cyclohexyl)-3,4-piperidine) ([^{3}H]TCP; 45 Ci/mmol) was obtained from PerkinElmer Life Sciences Products, Inc. (Boston, MA, USA), and stored

in ethanol at −20°C. [^{3}H]Ibogaine (23 Ci/mmol), ibogaine hydrochloride, and phencyclidine hydrochloride (PCP) were obtained through the National Institute on Drug Abuse (NIDA) (NIH, Baltimore, USA). (±)-Epibatidine was purchased form Sigma (Buchs, Switzerland). (−)-Nicotine tartrate, sodium cholate, polyethylenimine, leupeptin, bacitracin, pepstatin A, aprotinin, benzamidine, phenyl-methylsulfonyl fluoride (PMSF), and sodium azide were purchased from Sigma Chemical Co. (St. Louis, MO, USA). Geneticin and hygromycine B were obtained from Tocris Bioscience (Ellisville, MO, USA). κ-Bungarotoxin (κ-BTx) was obtained from Biotoxins Incorporated (St. Cloud, FL, USA). Fetal bovine serum and trypsin/EDTA were purchased form Gibco BRL (Paisley, UK). Salts were of analytical grade.

2.2. HEK293-hα3β4 cell culturing

HEK293-hα3β4 cells were the same as those used previously (Michelmore et al., 2002; Arias et al., 2010b). Cells were cultured in a 1:1 mixture of Dulbecco's Modified Eagle Medium containing 3.7g/L$NaHCO_3$,1.0g/L sucrose, with stable glutamine (L-alanyl-L-glutamine, 524 mg/L) and Ham's F-12 Nutrient Mixture comprising of 1.176 g/L $NaHCO_3$ with 10% (v/v) fetal bovine serum, geneticin (0.2 mg/mL), and hygromycine B (0.2 mg/mL), at 37 °C, 5% CO_2, and 95% relative humidity. The cells were passaged every 3 days by detaching the cells from the cell culture flask by washing with phosphate-buffered saline and brief incubation (~3 min) with trypsin (0.5 mg/mL)/EDTA (0.2 mg/mL).

2.3. Preparation of AChR membranes from HEK293-hα3β4 cells

To prepare HEK293-hα3β4 membranes in large quantities, the method described in Arias et al. (2009, 2010b) was used. In order to culture cells in suspension, non-treated Petri dishes (150 mm × 15 mm) were used. After culturing the cells for ~2–3 weeks, cells were harvested by gently scraping and centrifuged at 1000rpm for 5min at 4°C using a Sorvall Super T21 centrifuge. Cells were re-suspended in binding saline (BS) buffer (50 mM Tris-HCl, 120mM NaCl, 5mM KCl, 2mM $CaCl_2$, 1 mM $MgCl_2$, pH 7.4), containing 0.025% (w/v) sodium azide and a cocktail of protease inhibitors including, leupeptin, bacitracin, pepstatin A, aprotinin, benzamidine, and PMSF, as previously described. The suspension was maintained on ice and homogenized using a Polytron PT3000 (Brinkmann Instruments Inc., Westbury, NY, USA), and then centrifuged at 10,000 rpm for 30 min at 4°C. The pellet was finally resuspended in BS buffer containing 20% sucrose (w/v) using the Polytron, and briefly (5 × 15 s) sonicated (Branson Ultrasonics Co., Danbury, CT, USA) to assure maximum homogenization. HEK293-hα3β4 membranes were frozen at −80°C until required. Total protein was determined using the bicin-choninic acid protein assay (Thermo Fisher Scientific, Rockford, IL, USA).

2.4. Preparation of the cellular membrane affinity chromatography (CMAC) column and chromatographic system

The CMAC-hα3β4 AChR column was prepared by the immobilization of solubilized hα3β4 AChR membranes following a previously described protocol (Moaddel et al., 2005). HEK293-hα3β4 cells were homogenized basically as described in Section 2.3 in 10mL of buffer A (50 mM Tris-HCl buffer, pH 7.4, containing 20 μM leupeptin, 3mM benzamidine, 2mM $MgCl_2$, 3 mM $CaCl_2$, 5 mM KCl,100mM NaCl, 0.2mM PMSF, and 5mM EDTA), and subsequently solubilized in 10mL of buffer A containing 2% (w/v) sodium cholate. Then,

200 mg of the Immobilized Artificial Mono-layer (IAM) liquid chromatographic stationary phase (ID = 12μm, 300 Å pore) (Regis Technologies, Inc., Morton Grove, IL, USA) was suspended in the supernatant, and the mixture was rotated at room temperature (RT) for 1 h. The suspension was dialyzed for 1 day against 1 L of 50 mM Tris-saline buffer, pH 7.4, containing 5mM EDTA, 100mM NaCl, 0.1 mM $CaCl_2$, and 0.1 mM PMSF. While dialyzing, the detergent concentration decreases below the critical micelle concentration (CMC) and forces the adsorption of the membrane fragment onto the IAM stationary phase (Moaddel and Wainer, 2009). The suspension was then centrifuged at 700 × g at 4°C and the pellet (hα3β4-IAM) was washed three times with 10mM ammonium acetate buffer, pH 7.4. Finally, the stationary phase was packed into a HR 5/2 column (GE Healthcare, Piscataway, NJ, USA) to yield a 150 mm × 5 mm (ID) chromatographic bed, the CMAC-hα3β4 AChR column.

The CMAC-hα3β4 AChR column was then attached to the chromatographic system Series 1100 Liquid Chromatography/Mass Selective Detector (Agilent Technologies, Palo Alto, CA, USA) equipped with a vacuum de-gasser (G 1322 A), a binary pump (1312 A), an autosampler (G1313 A) with a 20 μL injection loop, a mass selective detector (G1946 B) supplied with atmospheric pressure ionization electrospray and an on-line nitrogen generation system (Whatman, Haverhill, MA, USA). The chromatographic system was interfaced to a 250 MHz Kayak XA computer (Hewlett-Packard, Palo Alto, CA, USA) running ChemStation software (Rev B.10.00, Hewlett-Packard).

10μL samples of 10 μM ibogaine were injected onto the CMAC-hα3β4 AChR column, and ligands were monitored in the positive ion mode using single ion monitoring at *m/z* = 310.9 $[MW+H]^+$ ion, with the capillary voltage at 3000 V, the nebulizer pressure at 35 psi, and the drying gas flow at 11 L/min at a temperature of 350°C.

2.5. Ca^{2+} influx measurements in HEK293-hα3β4 cells

Ca^{2+} influx was determined as previously described (Michelmore et al., 2002; Arias et al., 2009, 2010b). Briefly, 5×10^4 HEK293-hα3β4 cells per well were seeded 72 h prior to the experiment on black 96-well plates (Costar, New York, USA) and incubated at 37 °C in a humidified atmosphere (5% CO_2/95% air). 16–24h before the experiment, the medium was changed to 1% FBS in HEPES-buffered salt solution (HBSS) (130 mM NaCl, 5.4 mM KCl, 2mM $CaCl_2$, 0.8mM $MgSO_4$, 0.9mM NaH_2PO_4, 25mM glucose, 20 mM Hepes, pH 7.4). On the day of the experiment, the medium was removed by flicking the plates and replaced with 100μL HBSS/1% BSA containing 2 μM Fluo-4 (Molecular Probes, Eugene, Oregon, USA) in the presence of 2.5mM probenecid (Sigma, Buchs, Switzerland). The cells were then incubated at 37°C in a humidified atmosphere (5% CO_2/95% air) for 1 h. Plates were flicked to remove excess of Fluo-4, washed twice with HBSS/1% BSA, and finally refilled with 100μL of HBSS containing different concentrations of ibogaine or PCP, and preincubated for 5min. Plates were then placed in the cell plate stage of the fluorescent imaging plate reader (FLIPR) (Molecular Devices, Sunnyvale, CA, USA). A baseline consisting of 5 measurements of 0.4 s each was recorded. (±)-Epibatidine (0.1 μM) was then added from the agonist plate (placed in the agonist plate stage of the FLIPR) to the cell plate using the FLIPR 96-tip pipettor simultaneously to fluorescence recordings for a total length of 3 min.

The laser excitation and emission wavelengths are 488 and 510 nm, at 1 W, and a CCD camera opening of 0.4 s.

2.6. Equilibrium binding of[^{3}H]ibogaine to hα3β4 AChR membranes

In order to determine the binding affinity of [^{3}H]ibogaine for the hα3β4 AChR, equilibrium binding assays were performed as previously described (Arias et al., 2003, 2010b). Briefly, HEK293-hα3β4 AChR native membranes (1.8 mg/mL) were suspended in BS buffer. The total volume of the membrane suspensions (total and nonspecific binding) was divided into aliquots and increasing concentrations of [^{3}H]ibogaine + ibogaine (i.e., 0.2 nM–1.7 μM) were added to each tube and incubated for 2 h at RT. Total binding was obtained in the absence of ibogaine and nonspecific binding was determined in the presence of 100μM ibogaine. Specific binding was calculated as total binding minus nonspecific binding. AChR-bound [^{3}H]ibogaine was then separated from free ligand by a filtration assay using a 48-sample harvester system with GF/B Whatman filters (Brandel Inc., Gaithersburg, MD, USA), previously soaked with 0.5% polyethylenimine for 30 min. The membrane-containing filters were transferred to scintillation vials with 3mL of Bio-Safe II (Research Product International Corp., Mount Prospect, IL, USA), and the radioactivity was determined using a Beckman 6500 scintillation counter (Beckman Coulter, Inc., Fullerton, CA, USA).

Using the Prism software (GraphPad Software, San Diego, CA, USA), binding data were fitted according to the Rosenthal–Scatchard plot (Scatchard, 1949) using the equation:

$$\frac{[\mathrm{B}]}{[\mathrm{F}]} = -\left(\frac{[\mathrm{B}]}{K_\mathrm{d}}\right) + \left(\frac{B_\mathrm{max}}{K_\mathrm{d}}\right) \quad (1)$$

where the dissociation constant (K_d) for [^{3}H]ibogaine is obtained from the negative reciprocal of the slope. The specific activity of ibogaine binding sites in the membrane preparation can be estimated from the *x*-intersect (when $y = 0$) of the plot [B]/[F] *versus* [B], where the obtained value corresponds to the number of ibogaine binding sites (B_{max}) per the used concentration of total proteins (1.8mg/mL).

2.7. Radioligand competition binding experiments using hα3β4 AChRs in different conformational states

We studied the influence of ibogaine and PCP on either [^{3}H]ibogaine or [^{3}H]TCP binding to hα3β4 AChRs in different conformational states. In this regard, HEK293-hα3β4 AChR membranes (1.5mg/mL) were suspended in BS buffer with 20nM [^{3}H]ibogaine or 40nM [^{3}H]TCP in the absence (AChRs are mainly in the resting state; Arias et al., 2010b) or in the presence of 1 μM (−)-nicotine (desensitized/nicotine-bound state), and preincubated for 30 min at RT. Considering the K_d of ibogaine (see Fig. 2), nonspecific binding was determined in the presence of 100 μM ibogaine. The total volume was divided into aliquots, and increasing concentrations of the ligand under study were added to each tube and incubated for 2 h at RT. AChR-bound radioligand was then separated from free ligand by the filtration assay described above.

The concentration-response data were curve-fitted by nonlinear least-squares analysis using the Prism software. The corresponding IC_{50} values were calculated using the following equation:

$$\theta = \frac{1}{l + ([L]/IC_{50})^{n_H}} \quad (2)$$

where θ is the fractional amount of the radioligand bound in the presence of inhibitor at a concentration [L] compared to the amount of the radioligand bound in the absence of inhibitor (total binding). IC_{50} is the inhibitor concentration at which $\theta = 0.5$ (50% bound), and n_H is the Hill coefficient. The IC_{50} and n_H values obtained from the [^{3}H]TCP competition experiments were summarized in Table 2.

Taking into account that the hα3β4 AChR has a single population of [^{3}H]ibogaine binding sites (see Fig. 2), the observed IC_{50} values from the competition experiments described above were transformed into inhibition constant (K_i) values using the Cheng–Prusoff relationship (Cheng and Prusoff, 1973):

$$K_i = \frac{IC_{50}}{\{1 + ([NCA]/K_d^{NCA})\}} \quad (3)$$

where [NCA] is the initial concentration of [^{3}H]ibogaine, and K_d^{NCA} is the dissociation constant for [^{3}H]ibogaine (0.46 μM in the resting state; see Fig. 2). Since the affinity of PCP for the hα3β4 AChR is very low (see Table 2), a Scatchard plot for [^{3}H]TCP was not determined. Thus, to calculate the K_i values for ibogaine and PCP from the [^{3}H]TCP competition experiments in the resting state, the PCP K_i (see Table 2) was used as the K_d value. The calculated K_i values for the NCAs were summarized in Table 2.

2.8. Determination of the binding kinetics for ibogaine by non-linear chromatography

The binding kinetics parameters for ibogaine were determined by non-linear chromatography. The details of this approach and its application to the determination of the binding kinetics of NCAs to neuronal AChRs were presented earlier (Jozwiak et al., 2004; Moaddel et al., 2007). Chromatographic elutions of ibogaine from the CMAC-hα3β4 AChR column were carried out using a mobile phase composed of 10mM ammonium acetate buffer (pH 7.4):methanol (85:15, v/v) delivered at a flow rate of 0.2 mL/min at 20°C.

Previous experiments indicated that upon immobilization the AChR is mainly in the resting state, and it is necessary for the pharmacological action of an agonist to convert the AChR to the desensitized state (Moaddel et al., 2005). In this regard, the first set of experiments was performed in the presence of 1 nM κ-BTx (the AChR is mainly in the resting state). κ-BTx is a competitive antagonist member of the three-fingered neurotoxin family that maintains the AChR in the resting state (Moore and McCarthy, 1995). The CMAC-hα3β4 AChR column was equilibrated by passing the mobile phase with κ-BTx through the column for 1 h. Using a fresh column, ibogaine elutions were performed in parallel in the presence of 0.1 μM (±)-epibatidine (the AChR is mainly in the desensitized state).

In the non-linear chromatography approach, concentration-dependent asymmetric chromatographic traces are observed due to slow adsorption/desorption rates. The mathematical approach used in this study to resolve these non-linear conditions was the Impulse Input Solution (Wade et al, 1987). The chromatographic data were analyzed using PeakFit v4.12 for Windows Software (SPSS Inc., Chicago, IL, USA) following a previously reported protocol (Jozwiak et al., 2004). Briefly, the resultant peaks were fitted to the Impulse Input Solution model by adjusting four variables, namely a_0–a_3. The a_2 variable was directly used for the calculation of the dissociation rate constant (k_{off}) according to this equation:

$$k_{off} = \frac{1}{a_2 t_0} \quad (4)$$

where t_0 is the dead time of the column. The a_3 value was used to calculate the association constant (K_a) for the formation of the ligand-receptor complex in equilibrium using this relationship:

$$K_a = \frac{a_3}{[\text{ibogaine}]} \quad (5)$$

where [ibogaine] is the concentration of ibogaine. Both values can be used to further calculate the association rate constant k_{on} ($k_{on} = K_a \cdot k_{off}$).In addition, the free energy change (ΔG) for the interaction of the NCA with the receptor was determined as (reviewed in Arias, 2001):

$$\Delta G = -RT \ln K_a \quad (6)$$

where R is the gas constant (8.3145 $Jmol^{-1}$ K^{-1}), and T is the experimental temperature in kelvin (293 K).

2.9. Thermodynamic parameters of ibogaine interacting with the hα3β4 AChR

Chromatographic elutions of ibogaine from the CMAC-hα3β4 AChR column were carried out as explained in Section 2.8 at 10, 12, 16, 20 and 25 °C, respectively. The first set of experiments was performed in the presence of 1 nM κ-BTx (the receptor is mainly in the resting state; see Moore and McCarthy, 1995). A second set of experiments was conducted in the presence of 0.1 μM (±)-epibatidine (the AChR is mainly in the desensitized state).

The thermodynamic parameters were calculated from the chromatographic retention data at the experimental temperatures using the van't Hoff regression equation (reviewed in Arias, 2001):

$$\ln K_a = \left(\frac{\Delta S^\circ}{R}\right) - \left(\frac{\Delta H^\circ}{R}\right)\left(\frac{1}{T}\right) \quad (7)$$

where $\Delta S°$ and $\Delta H°$ are the standard entropy change and standard enthalpy change, respectively. These parameters were calculated using the slope ($\Delta H° = -\text{Slope} \cdot R$) and y-intersect ($\Delta S° = y\text{-intersect} \cdot R$) values from the plots. In addition, the entropic contribution

was calculated as $-T\Delta S°$, and the free energy change at 293 K (ΔG^{20}) was calculated using the Gibbs–Helmholtz equation (reviewed in Arias, 2001):

$$\Delta G^{20} = \Delta H^{\circ} - T\Delta S^{\circ} \quad (8)$$

The k_{off} values obtained using Eq. (5) were also used to construct the Arrhenius plots to determine the energy of activation (E_a) of the dissociation process, according to the Arrhenius equation (reviewed in Arias, 2001):

$$\ln k_{off} = \ln A - \left(\frac{E_a}{R}\right)\left(\frac{1}{T}\right) \quad (9)$$

where A is the Arrhenius or pre-exponential factor, and E_a was determined from the slope of the plot ($E_a = -\text{Slope}\cdot R$). In turn, the E_a values were used to calculate the enthalpy change of the transition state (ΔH^{+}) according to the following equation (reviewed in Arias, 2001):

$$\Delta H^{+} = E_a - RT \quad (10)$$

2.10. Molecular docking of ibogaine and PCP within the hα3β4 AChR ion channel

Since the absolute numbering of amino acid residues varies greatly between AChR subunits, the residues in the M2 transmembrane segments from the α3 and β4 subunits are referred here using the prime nomenclature (1′ to 20′), corresponding to residues Met^{243} to Glu^{262} from the *Torpedo* α1 subunit. A model of the hα3 β4 AChR was constructed using homology/comparative modeling method with the *Torpedo* AChR structure (PDB ID 2BG9), determined at ~4Å resolution by cryo-electron microscopy (Unwin, 2005; Miyazawa et al., 2003), as a template.

Computational simulations were performed using the same protocol as recently reported (Sanghvi et al., 2008; Arias et al., 2009, 2010b,c). In the first step, the ibogaine and PCP molecules in the neutral and protonated states were prepared using HyperChem 6.0 (HyperCube Inc., Gainesville, FL, USA). Sketched molecules were optimized using the semiempirical method AM1 (Polak-Ribiere algorithm to a gradient lower than 0.1 kcal/Å/mol) and then transferred for the subsequent step of ligand docking. The Molegro Virtual Docker (MVD 2008.2.4.0 Molegro ApS Aarhus, Denmark) was used for docking simulations of flexible ligands into the rigid target AChR model. In this step the complete structures of target receptors were used. The docking space was limited and centered on the middle of the ion channel and extended enough to ensure covering of the whole channel domain for sampling simulations (docking space was defined as a sphere of 21 Å in diameter). The actual docking simulations were performed using the following settings: numbers of runs = 100; maximal number of iterations = 10,000; maximal number of poses = 10, and the pose representing the lowest value of the scoring function (MolDockScore) for ibogaine and PCP was further analyzed.

3. Results

3.1. Inhibition of (±)-epibatidine-mediated Ca^{2+} influx in HEK293-hα3β4 cells by ibogaine and PCP

The potency of (±)-epibatidine to activate the hα3β4 AChR was first determined by assessing the fluorescence change in HEK293-hα3β4 cells after (±)-epibatidine stimulation. The observed EC_{50} value (19 ± 7nM; n_H= 1.21 ± 0.06; see Fig. 1) is in the same concentration range as other determinations using cell lines expressing the α3β4 AChR (Michelmore et al., 2002; Xiao et al., 1998; Arias et al., 2010b). (±)-Epibatidine-induced hα3β4 AChR activation is blocked by pre-incubation with ibogaine with an IC_{50} value (0.95 ±0.13 μM) ~9-fold lower than that for PCP (Table 1).The fact that the n_H values are close to unity (Table 1) indicates that the blocking process mediated by ibogaine and PCP is produced in a non-cooperative manner. In turn, this suggests that there is a single binding site for either ibogaine or PCP.

3.2. Equilibrium binding of[^{3}H]ibogaine to the hα3β4 AChR

In a first attempt to study the interaction of ibogaine with the hα3β4 AChR ion channel, the affinity of [^{3}H]ibogaine binding to HEK293-hα3β4 AChR membranes was determined. Fig. 2A shows the total (in the absence of ibogaine), nonspecific (in the presence of 100μM ibogaine), and specific (total – nonspecific) [^{3}H]ibogaine binding to hα3β4 AChR membranes in the resting (no ligand) state. Fig. 2B shows the Rosenthal-Scatchard plot for this specific binding. The results indicate that the HEK293-hα3β4 membranes have a single population of [^{3}H]ibogaine binding sites of relatively high affinity (K_d = 0.46 ± 0.06 μM) and specific activity of 3.9 ± 0.4 pmol/mg protein. Considering that there are two epibatidine binding sites and one ibogaine binding site per α3β4 AChR, the observed specific activity is practically the same as that obtained by [^{3}H]epibatidine equilibrium binding (8.9 pmol/mg protein; Xiao et al., 1998).

3.3. Radioligand binding competition experiments using ha3β4 AChRs in different conformational states

In order to compare the interaction of ibogaine and PCP with the hα3β4 AChR, the influence of each NCA on[^{3}H]ibogaine (Fig. 3) and [^{3}H]TCP binding (Fig. 4) to hα3β4 AChRs in the resting (no ligand) and desensitized/nicotine-bound states were determined. Previous studies indicated that the hα3β4 AChRs in the membrane preparation are mainly in the resting state (Arias et al., 2010b). Both NCAs inhibit ~100% the specific binding of [^{3}H]ibogaine (Fig. 3) and [^{3}H]TCP (Fig. 4) to either hα3β4 AChR state. Comparing the K_i values in different conformational states (Table 2), we can indicate that ibogaine binds to the desensitized/nicotine-bound hα3β4 AChR ion channel with slightly, but statistically relevant ($p < 0.05$; two-tailed *t*-test), higher affinity (~2.8-fold) than that for the resting/no ligand AChR. Although the absolute values are higher, the same trend (~2.6-fold) is observed for ibogaine in the [^{3}H]TCP competition results (Table 2). In addition, PCP binds to the resting hα3β4 AChR with ~10–16 times lower affinity compared to that for ibogaine (see Table 2). The calculated n_H values are close to unity (Table 2), indicating that both NCAs inhibit either [^{3}H]TCP or [^{3}H]ibogaine binding in a non-cooperative manner. These data suggest

that either ibogaine or PCP interacts with a single binding site, and that both NCAs probably inhibit radioligand binding in a steric fashion.

3.4. Binding kinetic parameters for ibogaine determined by non-linear chromatography

Fig. 5A shows the asymmetric traces for ibogaine when it is eluted from the CMAC-hα3β4 AChR column. The data were used to determine the k_{off} and K_a values according to Eqs. (4) and Eqs. (5), respectively, and thus, to further calculate the k_{on} values for ibogaine when it binds to the hα3β4 AChR in different conformational states (see Table 3).

The results indicate that ibogaine binding to the AChR ion channel is not a diffusion-controlled reaction because the determined association rate constants (k_{on} ~10^5 M^{-1} s^{-1}) are approximately four orders of magnitude smaller than the typical values for diffusion-controlled reactions (~$10^9 M^{-1}$ s^{-1}). The observed decrease in the k_{on} constants can be explained by structural and orientational constrains in the ibogaine binding pocket. The results also indicate that the dissociation rate constant (k_{off}) of ibogaine was slightly slower (0.078 ± 0.002 s^{-1}) when the column was exposed to (±)-epibatidine (the AChR is mainly in the desensitized state) compared to that exposed to κ-BTx (the AChR is mainly in the resting state) (0.088 ± 0.001 s^{-1}). This result indicates that ibogaine is dissociated from the desensitized hα3β4 AChR ion channel at a slightly slower rate than that from the resting AChR ion channel.

In absolute terms, the kinetic results indicate that the drug affinity for the hα3β4 AChR (K_d = 1/K_a ~ 0.3 μM) corresponds very well with that obtained by [^{3}H]ibogaine binding experiments (Table 2).

3.5. Thermodynamic parameters for the interactions of ibogaine with the hα3β4 AChR

In previous studies, an increase in the temperature changed the chromatographic retention of several NCAs including dextromethorphan and levomethorphan (Jozwiak et al., 2003), and bupropion (Arias et al., 2009). Thus, the temperature-dependent results can then be analyzed using the van't Hoff plot (see Eq. (7)) to calculate the changes in enthalpy (ΔH°) and entropy (ΔS°) associated with the interactions of the ligand with the immobilized AChR. In this study, increasing temperatures produced significant changes in the retentions of ibogaine on the CMAC-hα3β4 AChR column in the presence of either κ-BTx (resting state; see Moore and McCarthy, 1995)or (±)-epibatidine (desensitized state), respectively (see Fig. 5B). Since the resulting van't Hoff plots were linear (Fig. 6A), the thermodynamic parameters ΔH° and ΔS° were calculated from the slopes and intercepts of the van't Hoff plots, respectively, according to Eq. (7), whereas ΔG^{20} was calculated according to Eq. (8) (Table 4). The linearity of van't Hoff plots indicates an invariant retention mechanism over the temperature range studied (Jozwiak et al., 2002, 2003).

The calculated thermodynamic parameters for ibogaine indicate that the entropic energetic contribution (−TΔS°) is higher than the enthalpic (ΔH°) contribution in both AChR states (Table 4). Moreover, this difference was slightly more pronounced in the desensitized state compared to that in the resting state (Table 4). This result suggests that ibogaine preferably induces local con-formational changes and/or solvent reorganization in the binding pocket of

the desensitized AChR. The fact that the $\Delta H°$ values are negative also suggests the existence of attractive forces (e.g., van der Waals, hydrogen bond, and electrostatic interactions) forming stable complexes in both conformational states. The calculated ΔG^{20} values (see Table 4) are in the same energetic range as those determined using the radioligand binding data (see Table 2).

Arrhenius plots were also constructed using the determined k_{off} values (see Eq. (4)) for ibogaine at different temperatures (Fig. 6B). Since the Arrhenius plots are different from zero, the drug dissociation process is mediated mainly by an enthalpic component. To quantify this component, the E_a values were first calculated from the Arrhenius plots, and the ΔH^+ values were subsequently calculated using Eq. (10) (Table 4). The fact that the E_a value in the desensitized state is higher than that in the resting state indicates that the energy barrier for drug dissociation from the desensitized ion channel is higher than that from the resting ion channel. This correlates well with a higher ΔH^+ value in the desensitized state compared to that in the resting state.

3.6. Molecular docking of ibogaine and PCP within the ha3β4 AChR ion channel

The main structural difference between the molecular model of the hα3β4 AChR ion channel domain and the corresponding domains of other receptor types is that the amino acid ring at position 13′ in the hα3β4 AChR ion channel has three phenylalanine residues, one on each β4 subunit (β4-Phe^{253}). In this regard, this ring is called the valine/phenylalanine ring. Phenylalanine residues are significantly bulkier than valine residues, and point directly to the center of the ion channel, changing considerably the binding properties of the NCAs interacting at this site. The importance of this structural feature was demonstrated earlier in docking simulations of a large cohort of compounds in the α3β4 AChR ion channel (Jozwiak et al., 2004; Arias et al., 2010b) in comparison to docking simulations in the α3β2 AChR system (Jozwiak et al., 2007).

Ibogaine and PCP structures, each in the neutral and protonated states, were docked in the hα3β4 AChR ion channel model obtained by means of comparative/homology modeling using the *Torpedo* AChR. Molegro Virtual Docker generated a series of docking poses and ranked them using energy-based criterion using the embedded scoring function in MolDockScore. Based on this ranking, the lowest energy pose of the hα3β4 AChR-ligand complex was selected and presented for ibogaine (Fig. 7) and PCP (Fig. 8), respectively. Comparison of the MolDockScore values for the best ranked complexes indicates that the docking of ibogaine generated poses of lower energy (−97.2 and −96.0 kJ/mol for neutral and protonated molecule, respectively) than that obtained by PCP docking (−87.0 and −85.7 kJ/mol, respectively). This result is in agreement with the binding (see Table 2) and functional (see Table 1) results indicating that ibogaine presents higher affinity and is more potent than PCP.

The modeling results suggest that the docking poses is essentially the same for the neutral and protonated states of either ibogaine or PCP. This notion is supported by the calculated MolDockScore values indicating that the complexes present similar scores in the neutral and protonated states. Detailed analyses of the complexes show that the docked molecule interacts only with M2 helices, provided by each subunit. Both ibogaine and PCP interact

within the middle portion of the ion channel in the cavity formed between the valine/phenylalanine (position 13′) and serine (position 6′) rings. Since the three β4-Phe^{253} residues forming the valine/phenylalanine ring change significantly the structure of the binding site, both ligands interact with a large hydrophobic cleft formed by the phenylalanine and valine residues and thus, the contact distance is significantly closer compared to that with the valine ring (position 13′) in the muscle AChR ion channel (Arias et al., 2009). This unique mode of binding can be easily observed in the ibogaine (Fig. 7) and PCP (Fig. 8) simulations, where the aliphatic ring systems of each drug interact by van der Waals contacts with the valine/phenylalanine ring. Ibogaine can also form hydrogen bonds between its methoxy moiety and serine residues at the serine ring (position 6′), and van der Waals interactions with the leucine ring (position 9′) (Fig. 7B). The distance between the oxygen atom in the ibogaine methoxy moiety and two of the closest hydroxyl groups, one from the α3-Ser247 residue and another from the adjacent β4-Ser246 residue, is ~3 Å in both cases. On the other hand, PCP forms additional van der Waals interactions with the serine and leucine rings, and no hydrogen bond is apparent (Fig. 8B).

4. Discussion

Previous studies using animal models of drug addiction indicate that ibogaine and its analogs have anti-addictive properties (Glick and Maisonneuve, 1998; Glick et al., 2000, 2002, 2008; Pace et al., 2004; Taraschenko et al., 2005). In addition, this pharmacological activity seems to be mediated, at least partially, by their noncompetitive inhibitory action on several AChRs, including the α3β4 subtype (Fryer and Lukas, 1999; Badio et al., 1997; Glick et al., 2000; Pace et al., 2004; Arias et al., 2010c).

There are at least two approaches that can be used to develop better and safer drugs: (1) using a molecule as an initial scaffold that can be improved by further structural refinements, and where the activity and specificity of the new analogs can be subsequently tested, the so-called “lead” approach and/or, (2) synthesizing a wide set of new analogs based on the structural requirements of the binding pocket for a model molecule in a particular target receptor, the so-called “hit” approach. In this regard, we want to characterize the ibogaine binding site in the hα3β4 AChR by comparing the pharmacological activity of ibogaine with that for PCP on hα3β4 AChRs in distinct conformational states. To this end, radioligand binding and Ca^{2+} influx assays, thermodynamic and kinetic measurements, and molecular docking studies are performed.

4.1. Ligand interaction with the agonist-activated AChR ion channel

To compare the effect of ibogaine and PCP on (±)-epibatidine-activated Ca^{2+} influx in HEK293-hα3β4 cells, a pre-incubation protocol was used (Fig. 1). The results indicated that ibogaine is ~9-fold more potent than PCP in inhibiting the hα3β4 AChR ion channel. A similar result was obtained by $^{86}Rb^{+}$ efflux experiments in neuroblastoma SH-SY5Y cells (Fryer and Lukas, 1999). These cells resemble human fetal sympathetic neurons grown in primary culture and express the α3, α4, α7, β2, and β4 subunits (Groot Kormelink and Luyten, 1997). On the protein level, they express the α7 homopentamer and further, α3-containing AChRs of at least two subtypes, half of which containing β2 subunits (Wang et

al., 1996). In contrast to the results in the present study with the HEK293-hα3β4 cells where only the hα3α4 AChR is expressed, the effects in the SH-SY5Y cells are caused by the concerted activation of several different endogenously expressed AChRs. In addition, the observed PCP IC_{50} value (8.5 ± 1.4 μM) is statistically the same as that obtained by $^{86}Rb^{+}$ efflux experiments in rat α3β4 AChRs (7.0 ± 1.3 μM; Hernandez et al., 2000), indicating that PCP inhibits both human and rat α3β4 AChRs with the same potency.

Pre-clinical studies performed in Glick's laboratory indicate that a low dose of 18-methoxycoronaridine (an ibogaine analog), that it is ineffective alone, in combination with low dose of either mecamylamine (a noncompetitive antagonist of several AChRs with anti-addictive properties) (Glick et al., 2000, 2002), dextromethorphan (a NMDA receptor blocker) (Glick et al., 2002; Taraschenko et al., 2005), or the antidepressant and anti-nicotinic drug bupropion (Taraschenko et al, 2005; reviewed in Arias, 2009), reduces the addictive action of several drugs of abuse in rats. Interestingly, these compounds have relatively higher specificity for α3β4 AChRs compared to other neuronal AChRs (Glick et al., 2002; Taraschenko et al., 2005). These results point out the importance of α3β4 AChRs expressed in the brain, more specifically in the medial habenula, interpeduncular nucleus, ventral tegmental area, dorsolateral tegmentum, basolateral amygdale, locus coeruleus, and hippocampus (Glick et al., 2008; reviewed in Gotti et al., 2006), for the therapeutic actions of ibogaine analogs, especially considering that some of these brain areas are involved in drug addiction (Glick et al, 2002, 2008; Taraschenko et al., 2005; reviewed in Gotti et al., 2006; Glick et al., 2000; Arias, 2009).

4.2. Characterization of the ibogaine binding site

The results from the Scatchard-type analysis (K_d ~0.5 μM; Fig. 2) and from the radioligand competition binding experiments (K_i ~0.4-1 μM; Table 2) indicate that ibogaine binds to a single binding site in the hα3β4 AChR ion channel with relatively high affinity. To our knowledge, this is the first time that a direct interaction of ibogaine with the hα3β4 AChR ion channel is demonstrated by radioligand binding methods. The results from the radioligand competition binding experiments also indicate that ibogaine binds to the desensitized hα3β4 AChR with higher affinity than that for the resting AChR (see Table 2). This is explained by the kinetic results indicating that ibogaine dissociates more slowly from the desensitized hα3β4 AChR ion channel than from the resting ion channel (Table 3). Previous results using the *Torpedo* AChR also indicate that ibogaine binds with higher affinity to the desensitized AChR compared with that for the resting AChR (Arias et al., 2010c).

The radioligand competition experiments also indicate that ibogaine binds to the resting hα3β4 AChR ion channel with higher affinity than that for PCP (see Table 2), indicating that ibogaine might be a more effective NCA than PCP. In fact, our Ca^{2+} influx experiments support this conclusion (see Table 1). More importantly, ibogaine inhibits the binding of [^{3}H]TCP (the structural and functional analog of PCP) and vice versa, PCP inhibits the binding of [^{3}H]ibogaine to resting hα3β4 AChRs with n_H values close to unity (Table 2). Hill coefficients close to unity indicate a non-cooperative interaction between ibogaine and PCP, suggesting that each drug interacts with a single binding site in the resting hα3β4

AChR ion channel. This evidence suggests a steric mode of competition between ibogaine and PCP and thus, the existence of overlapping sites in the resting hα3β4 AChR ion channel. However, we do not have information of the exact location of the PCP and ibogaine binding site(s) in the hα3β4 AChR ion channel. To address this question, the location of the ibogaine and PCP binding sites were additionally studied by molecular docking. The structural analysis of the obtained molecular complexes suggests that both ibogaine (Fig. 7) and PCP (Fig. 8) interact within the middle portion of the hα3β4 AChR ion channel in the cavity formed between the valine/phenylalanine (position 13′) and serine (position 6′) rings. These results support our competition experiments (see Fig. 3 and Table 2), indicating that potentially there is a binding site for ibogaine analogs that overlaps the PCP locus in the hα3β4 AChR ion channel. These results also concur with previous experiments showing that tricyclic antidepressants bind to a luminal domain between the valine/phenylalanine (position 13′) and leucine (position 9') rings (Arias et al., 2010b).

As a first approximation, the binding site location for PCP in the hα3β4 AChR ion channel is similar to that observed in the muscle-type AChR ion channel (Sanghvi et al., 2008; Hamouda et al., 2008). PCP binds in a domain formed between the serine (position 6′) and valine (position 13′) rings in the *Torpedo* AChR ion channel mainly by van der Waals interactions (Sanghvi et al., 2008), in agreement with the current docking results on the hα3β4 AChR system (see Fig. 8B). The evidence suggesting that the PCP binding location in the hα3β4 AChR ion channel is not dependent on the ionization state (Fig. 8) has been also observed previously in muscle AChR ion channels (Sanghvi et al., 2008). This comparable binding site location and lack of ionic state dependence suggest a similar mode of PCP inhibition between both AChR types. However, the inhibitory potency of PCP in the hα3β4 AChR (see Table 1) is ~2-fold higher than that in the muscle AChR (Fryer and Lukas, 1999), suggesting that other structural components will be differentially involved in each ion channel type.

A more detailed analysis of the ibogaine docking results on the hα3β4 AChR shows that there are at least two main structural differences when compared with that for muscle AChR ion channels (Arias et al., 2010c). The first difference is that the binding site location for ibogaine in the hα3β4 AChR ion channel model does not depend on whether the molecule is in the neutral or protonated form (Fig. 7), whereas it depends on the muscle AChRs. The second difference is that ibogaine primarily binds to the valine/phenylalanine ring (position 13′) mainly by van der Waals contacts, and additional polar interactions occur with the serine ring (position 6′). This evidence is in agreement with the observed enthalpic component for the interaction of ibogaine with the hα3β4 AChR (see Table 3). However, the docking results contrast with previous studies in muscle-type AChRs where neutral ibogaine interacts primarily with the serine ring by a network of hydrogen bonds, and secondly with residues at the threonine (position 2′), leucine (position 9′), and valine (position 13′) rings by additional van der Waals contacts (Arias et al., 2010c). This indicates that the structural components involved in the interaction of ibogaine with the ion channel depend on the AChR subtype.

This study does not intend to determine directly the therapeutic properties of ibogaine and PCP. Instead, this work will pave the way for a better understanding of how these NCAs

interact with the hα3β4 AChR. In this regard, our data indicate that ibogaine functionally blocks agonist-induced hα3β4 AChR ion flux by binding with relatively high affinity to a single site in the ion channel. Molecular modeling results suggest that ibogaine and PCP interact with overlapping sites in a channel domain formed between the serine and valine/phenylalanine rings, which is shared with tricyclic antidepressants. Once in its locus, ibogaine dissociates slowly from the desensitized hα3β4 AChR ion channel, suggesting that this alkaloid might maintain the AChR in the desensitized state for longer time.

Acknowledgements

This research was supported by grants from the Science Foundation Arizona and Stardust Foundation and the Office of Research and Sponsored Programs, Midwestern University (to H.R.A.), by the FOCUS research subsidy from the Foundation for Polish Science (to K.J.). This research was also supported in part by the Intramural Research Program of the NIH, National Institute on Aging. The authors thank to National Institute on Drug Addiction (NIDA, NIH, Bethesda, Maryland, USA) for its gift of [^{3}H]Ibogaine, ibogaine, and phencyclidine, and to Paulina Iacoban for their technical assistance. Xiao Juan Yuan was supported by a Student Summer Fellowship, Western University of Health Sciences (Pomona, CA, USA).

Abbreviations

AChR	nicotinic acetylcholine receptor
NCA	noncompetitive antagonist
PCP	phencyclidine
[^{3}H]TCP	[piperidyl-3,4-^{3}H(N)]-(N-(1-(2 thienyl)cyclohexyl)-3,4-piperidine)
Ibogaine (or 12-methoxyibogamine)	7-ethyl-6,2,7,8,9,10,12,13-octahydro-2-methoxy-6,9-methano 5*H*-pyrido(1′,2′:1,2-azepine(4,5-)indole)
κ-BTx	κ-bungarotoxin
RT	room temperature
BS buffer	binding saline buffer
K_i	inhibition constant
K_d	dissociation constant
K_a	association constant
k_{off}	dissociation rate constant
k_{on}	association rate constant
IC_{50}	ligand concentration that produces 50% inhibition (of binding or of Ca^{2+} influx)
n_H	Hill coefficient
EC_{50}	agonist concentration that produces 50% AChR activation
DMEM	Dulbecco’s Modified Eagle Medium

FLIPR	fluorescent imaging plate reader
BSA	bovine serum albumin
PMSF	phenylmethylsulfonyl fluoride

References

Albuquerque EX, Pereira EFR, Alkondon A, Rogers SW. Mammalian nicotinic acetyl-choline receptors: from structure to function. Physiol Rev. 2009; 89:73–120. [PubMed: 19126755]

Arias, HR. Thermodynamics of nicotinic receptor interactions. In: Raffa, RB., editor. Drug-receptor thermodynamics: introduction and applications. USA: John Wiley & Sons, Ltd; 2001. p. 293-358.

Arias, HR. Ligand-gated ion channel receptor superfamilies. In: Arias, HR., editor. Biological and biophysical aspects of ligand-gated ion channel receptor super-families. Kerala, India: Research Signpost; 2006. p. 1-25.[Chapter 1]

Arias HR. Is the inhibition of nicotinic acetylcholine receptors by bupropion involved in its clinical actions? Int J Biochem Cell Biol. 2009; 41:2098–2108. [PubMed: 19497387]

Arias HR, Bhumireddy P, Bouzat C. Molecular mechanisms and binding site locations for noncompetitive antagonists of nicotinic acetylcholine receptors. Int J Biochem Cell Biol. 2006a; 38:1254–1276. [PubMed: 16520081]

Arias HR, Bhumireddy P, Spitzmaul G, Trudell JR, Bouzat C. Molecular mechanisms and binding site location for the noncompetitive antagonist crystal violet on nicotinic acetylcholine receptors. Biochemistry. 2006b; 45:2014–2026. [PubMed: 16475790]

Arias HR, Feuerbach D, Bhumireddy P, Ortells MO. Inhibitory mechanisms and binding site locations for serotonin selective reuptake inhibitors on nicotinic acetylcholine receptors. Int J Biochem Cell Biol. 2010a; 42:712–724. [PubMed: 20079457]

Arias HR, Feuerbach D, Targowska-Duda KM, Jozwiak K. Catharanthine alkaloids are noncompetitive antagonists of muscle nicotinic acetylcholine receptors. Int Neurochem. 2010c in press.

Arias HR, Targowska-Duda KM, Sullivan CJ, Feuerbach D, Maciejewski R, Jozwiak K. Different interaction between tricyclic antidepressants and mecamylamine with the human α3β4 nicotinic acetylcholine receptor. Int Neurochem. 2010b; 56:642–649.

Arias HR, Gumilar F, Rosenberg A, Targowska-Duda KM, Feuerbach D, Jozwiak K, et al. Interaction of bupropion with muscle-type nicotinic acetylcholine receptors in different conformational states. Biochemistry. 2009; 48:4506–4518. [PubMed: 19334677]

Arias HR, Trudell JR, Bayer EZ, Hester B, McCardy EA, Blanton MP. Noncompetitive antagonist binding sites in the *Torpedo* nicotinic acetylcholine receptor ion channel. Structure-activity relationship studies using adamantane derivatives. Biochemistry. 2003; 42:7358–7370. [PubMed: 12809491]

Badio B, Padgett WL, Daly JW. Ibogaine: a potent noncompetitive blocker of gan-glionic/neuronal nicotinic receptors. Mol Pharmacol. 1997; 51:1–5. [PubMed: 9016339]

Cheng Y, Prusoff WH. Relationship between the inhibition constant (K_i) and the concentration of inhibitor which causes 50 percent inhibition (IC_{50}) of an enzymatic reaction. Biochem Pharmacol. 1973; 22:3099–3108. [PubMed: 4202581]

Fryer JD, Lukas RJ. Noncompetitive functional inhibition at diverse, human nicotinic acetylcholine receptor subtypes by bupropion, phencyclidine, and ibogaine. J Pharmacol Exp Ther. 1999; 288:288–92.

Glick SD, Maisonneuve IM. Mechanisms of antiaddictive actions of ibogaine. Ann NY Acad Sci. 1998; 844:214–226. [PubMed: 9668680]

Glick SD, Maisonneuve IM, Kitchen BA, Fleck MW. Antagonism of α3β4 nicotinic receptors as a strategy to reduce opioid and stimulant self-administration. Eur J Pharmacol. 2002; 438:99–105. [PubMed: 11906717]

Glick SD, Maisonneuve IM, Szumlinski KK. 18-Methoxycoronaridine (18-MC) and ibogaine: comparison of antiaddictive efficacy, toxicity, and mechanisms of action. Ann NY Acad Sci. 2000; 914:369–386. [PubMed: 11085336]

Glick SD, Sell EM, Maisonneuve IM. Brain regions mediating α3β4 nicotinic antagonist effects of 18-MC on methamphetamine and sucrose self-administration. EurJ Pharmacol. 2008; 599:91–95. [PubMed: 18930043]

Gotti C, Zoli M, Clementi F. Brain nicotinic acetylcholine receptors: native subtypes and their relevance. Trends Pharm Sci. 2006; 27:482–491. [PubMed: 16876883]

Groot Kormelink PJ, Luyten WH. Cloning and sequence of full-length cDNAs encoding the human neuronal nicotinic acetylcholine receptor (nAChR) subunits β3 and β4 and expression of seven nAChR subunits in the human neuroblastoma cell line SH-SY5Y and/or IMR-32. FEBS Lett. 1997; 400:309–314. [PubMed: 9009220]

Hamouda AK, Chiara DC, Blanton MP, Cohen JB. Probing the structure of the affinity-purified and lipid-reconstituted *Torpedo* nicotinic acetylcholine receptor. Biochemistry. 2008; 47:12787–12794. [PubMed: 18991407]

Hernandez SC, Bertolino M, Xiao Y, Pringle KE, Caruso FS, Kellar KJ. Dextromethor-phan and its metabolite dextrorphan block α3β4 neuronal nicotinic receptors. J Pharmacol Exp Ther. 2000; 293:962–967. [PubMed: 10869398]

Jozwiak K, Haginaka J, Moaddel R, Wainer IW. Displacement and nonlinear chro-matographic techniques in the investigation of interaction of noncompetitive inhibitors with an immobilized α3β4 nicotinic acetylcholine receptor liquid chromatographic stationary phase. Anal Chem. 2002; 74:4618–4624. [PubMed: 12349962]

Jozwiak K, Hernandez S, Kellar KJ, Wainer IW. The enantioselective interactions of dextromethorphan and levomethorphan with the α3β4-nicotinic acetylcholine receptor: comparison of chromatographic and functional data. J Chromatogr B. 2003; 797:373–379.

Jozwiak K, Ravichandran S, Collins JR, Moaddel R, Wainer IW. Interaction of noncompetitive inhibitors with the α3β2 nicotinic acetylcholine receptor investigated by affinity chromatography and molecular docking. J Med Chem. 2007; 50:6279–6283. [PubMed: 17973360]

Jozwiak K, Ravichandran S, Collins JS, Wainer IW. Interaction of noncompetitive inhibitors with an immobilized α3β4 nicotinic acetylcholine receptor investigated by affinity chromatography, quantitative-structure activity relationship analysis, and molecular docking. J Med Chem. 2004; 47:4008–4021. [PubMed: 15267239]

Maisonneuve IM, Glick SD. Anti-addictive actions of an iboga alkaloid congener: a novel mechanism for a novel treatment. Pharmacol Biochem Behav. 2003; 75:607–618. [PubMed: 12895678]

Mansvelder HD, van Aerde KI, Couey JJ, Brussaard AB. Nicotinic modulation of neuronal network: from receptors to cognition. Psychopharmacology. 2006; 184:292–305. [PubMed: 16001117]

Michelmore S, Croskery K, Nozulak J, Hoyer D, Longato R, Weber A, et al. Study of the calcium dynamics of the human α4β2, α3β4 and α1β1γδ nicotinic acetylcholine receptors. Naunyn-Schmiedebergs Arch Pharmacol. 2002; 366:235–245. [PubMed: 12172706]

Miyazawa A, Fujiyoshi Y, Unwin N. Structure and gating mechanism ofthe acetylcholine receptor pore. Nature. 2003; 423:949–955. [PubMed: 12827192]

Moaddel R, Jozwiak K, Wainer IW. Allosteric modifiers of neuronal nicotinic receptors: new methods, new opportunities. Med Res Rev. 2007; 27:723–753. [PubMed: 17238157]

Moaddel R, Jozwiak K, Whittington K, Wainer IW. Conformational mobility of immobilized α3β2, α3β4, α4β2, α4β4 nicotinic acetylcholine receptors. Anal Chem. 2005; 77:895–901. [PubMed: 15679359]

Moaddel R, Wainer IW. The preparation and development of cellular membrane affinity chromatography columns. Nat Protocol. 2009; 4:197–205.

Moore MA, McCarthy MP. Snake venom toxins, unlike smaller antagonists, appear to stabilize a resting state conformation of the nicotinic acetylcholine receptor. Biochim Biophys Acta. 1995; 1235:336–342. [PubMed: 7756343]

Pace CJ, Glick SD, Maisonneuve IM, He LW, Jokiel PA, Kuehne ME, et al. Novel iboga alkaloid congeners block nicotinic receptors and reduce drug self-administration. Eur J Pharmacol. 2004; 492:159–167. [PubMed: 15178360]

Quick MW, Ceballos RM, Kasten M, McIntosh JM, Lester RAJ. a3b4 subunit-containing nicotinic receptors dominate function in rat medial habenula neurons. Neu-ropharmacology. 1999; 38:769–783.

Sanghvi M, Hamouda AK, Jozwiak K, Blanton MP, Trudell JR, Arias HR. Identifying the binding site(s) for antidepressants on the *Torpedo* nicotinic acetylcholine receptor: [^{3}H]2-Azidoimipramine photolabeling and molecular dynamics studies. Biochem Biophys Acta. 2008; 1778:2690–2699. [PubMed: 18817747]

Taraschenko OD, Panchal V, Maisonneuve IM, Glick SD. Is antagonism of α3β4 nicotinic receptors a strategy to reduce morphine dependence? Eur J Pharmacol. 2005; 513:207–218. [PubMed: 15862802]

Unwin N. Refined structure ofthe nicotinic acetylcholine receptor at 4Å resolution. J Mol Biol. 2005; 346:967–989. [PubMed: 15701510]

Vocci FJ, London ED. Assessment of neurotoxicity from potential medications for drug abuse: ibogaine testing and brain imaging. Ann NY Acad Sci. 1997; 820:829–839.

Wade JL, Bergold AF, Carr PW. Theoretical description of nonlinear chromatography, with applications to physicochemical measurements in affinity chromatography and implications for preparative-scale separations. Anal Chem. 1987; 59:1286–1295.

Wang F, Gerzanich V, Wells R, Anand R, Peng X, Keyser K, et al. Assembly of human neuronal nicotinic receptor α5 subunits with α3, β2, and β4 subunits. J Biol Chem. 1996; 271:17656–17665. [PubMed: 8663494]

Xiao Y, Meyer EL, Thompson JM, Surin A, Wroblewski J, Kellar KJ. Rat α3/β4 subtype of neuronal nicotinic acetylcholine receptor stably expressed in a transfected cell line: Pharmacology of ligand binding and function. Mol Pharmacol. 1998; 54:322–333. [PubMed: 9687574]

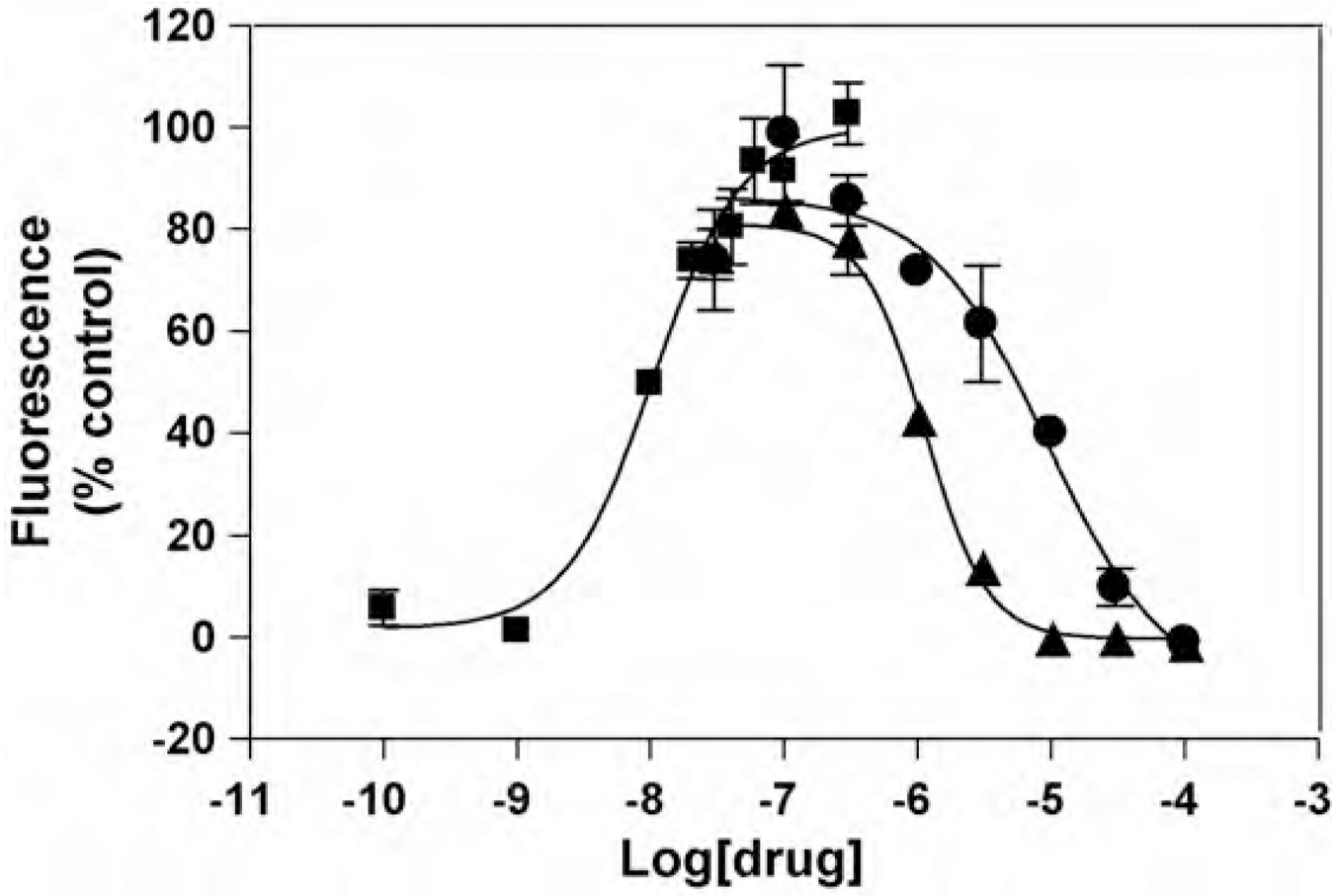

Fig. 1.

Effect of ibogaine and PCPon(±)-epibatidine-induced Ca^{2+} influx in HEK293 cells expressing hc3β4 AChRs. Increased concentrations of (±)-epibatidine (■) activate the hα3β4 AChR with potency EC_{50} =19±7nM (n_H = 1.21 ±0.06). Subsequently, cells were pre-treated with several concentrations of ibogaine (▲) and PCP (●), followed by addition of 0.1 μM (±)-epibatidine. Response was normalized to the maximal (±)-epibatidine response which was set as 100%. The plots are representative often (■), three (●), and five (▲) determinations, respectively, where the errorbars represent the standard deviations (S.D.). The calculated IC_{50} and n_H values are summarized in Table 1.

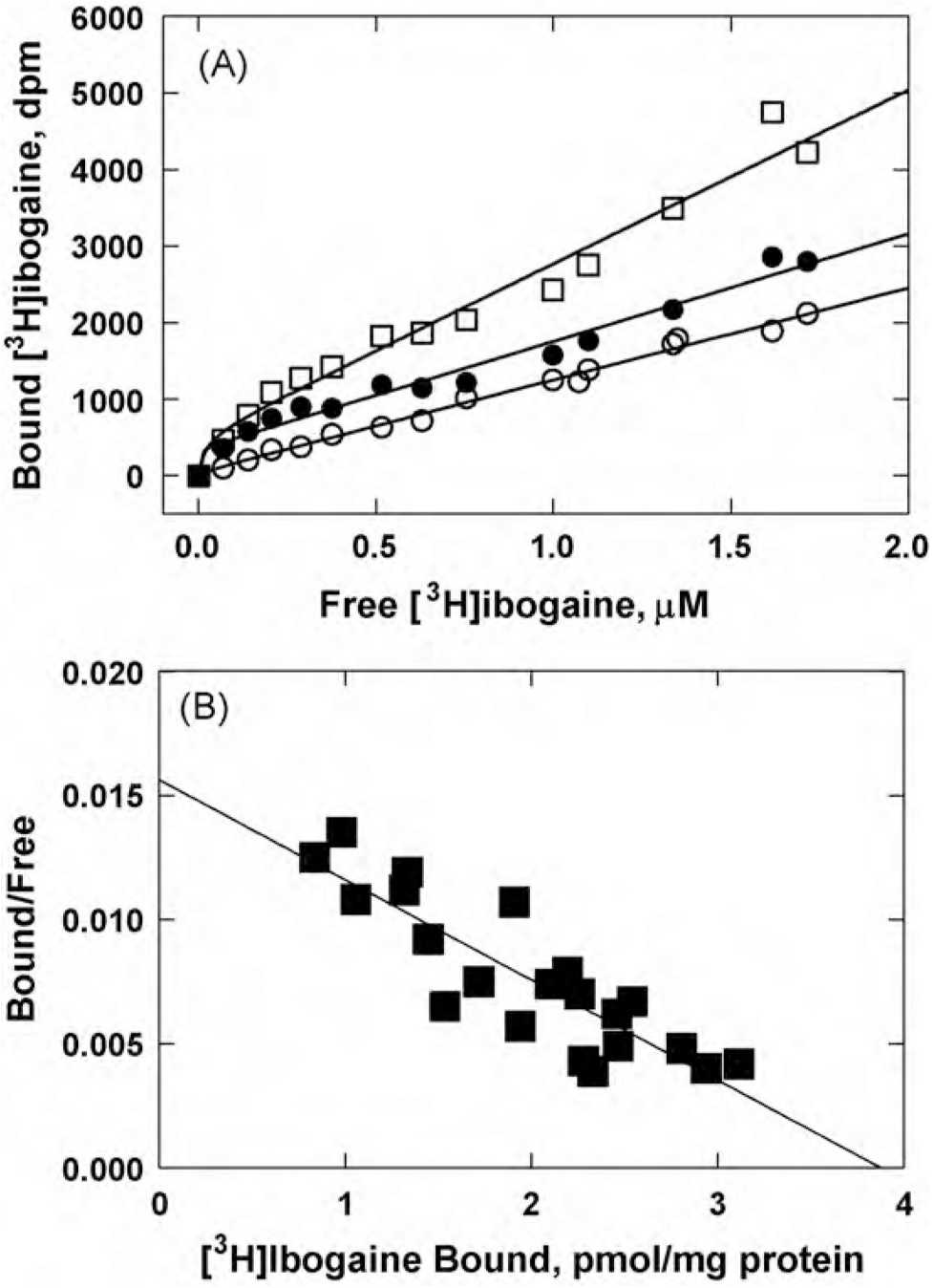

Fig. 2.

Equilibrium binding of [^{3}H]ibogaine to hα3β4 AChR membranes. (A) total (□), nonspecific (○) (in the presence of 100 μM ibogaine), and specific (●) (total - nonspecific binding) [^{3}H]ibogaine binding. hα3β4 AChR native membranes (1.8mg/mL) were suspended in BS buffer, and preincubated for 2h at RT. Then, the total volume of the membrane suspensions (total and nonspecific binding) was divided into aliquots and increasing concentrations of [^{3}H]ibogaine + ibogaine (i.e., 0.07–1.7 μM) were added to each tube. Finally, the AChR-bound [^{3}H]ibogaine was separated from the free ligand by using the filtration assay

described in Section 2.6. (B) Rosenthal-Scatchard plot for [^{3} H]ibogaine specific binding to the hα3β4 AChR ion channel. The K_d value (0.46 ± 0.06 μM) was determined from the negative reciprocal of the slope, according to Eq. (1). The specific activity (3.9 ± 0.4 pmol/mg protein) of the membrane was obtained from the *x*-intersect (when $y = 0$) of the plot [B]/[F] *versus* [B] according to Eq. (1). Shown is the combination of two separate experiments.

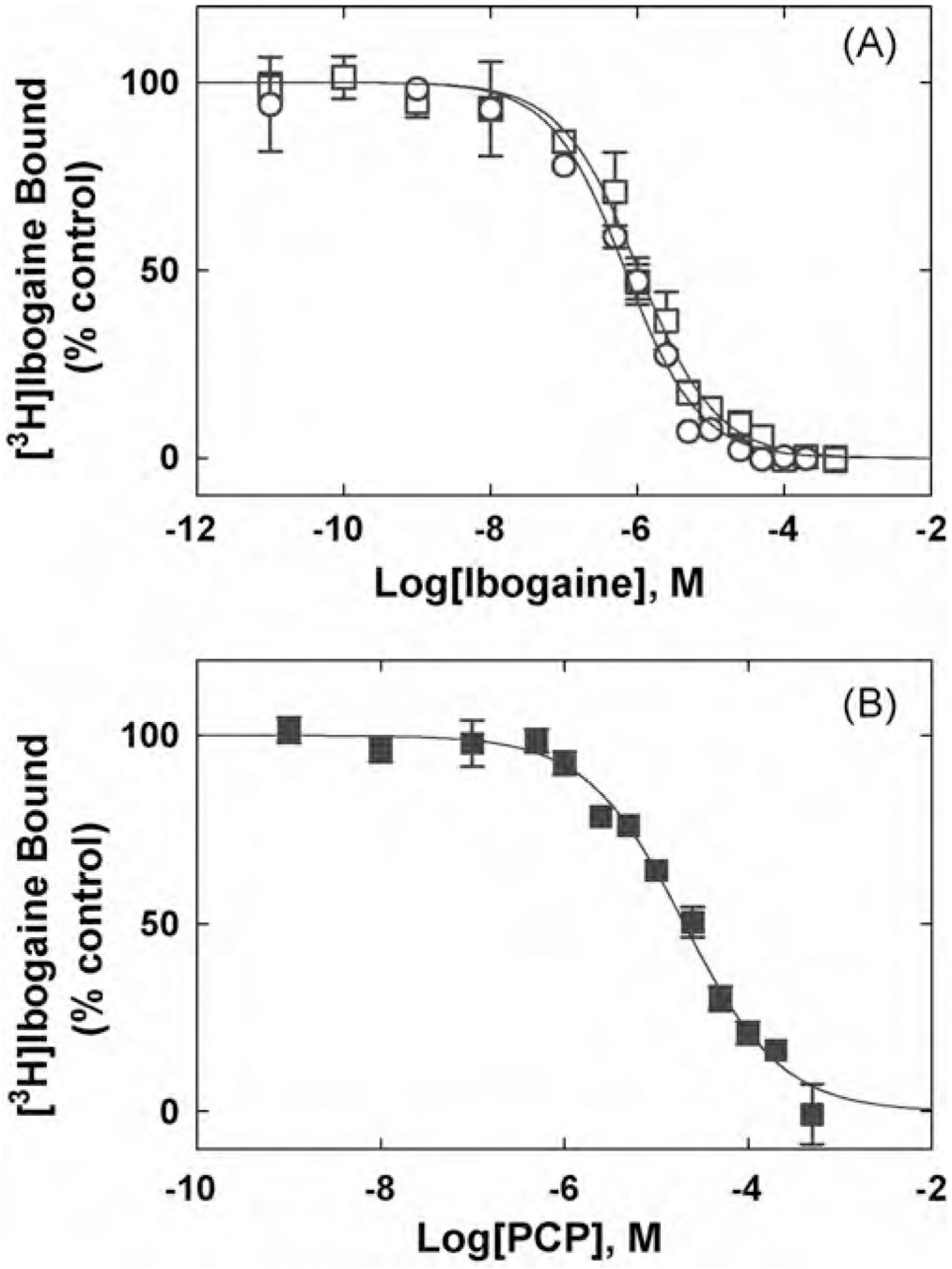

Fig. 3.

Inhibition of [^{3}H]ibogaine binding to hα3β4 AChRs in different conformational states elicited by (A) ibogaine and (B) PCP. hα3β4 AChR membranes (1.5 mg/mL) were equilibrated (2 h) with 20nM [^{3}H]ibogaine, in the absence (□,■) (AChRs are mainly in the resting state) or in the presence of 1μM (−)-nicotine (○) (AChRs are mainly in the desensitized state), and increasing concentrations of the competitor. Nonspecific binding was determined at 100μM ibogaine. From these plots the IC_{50} and n_H values were obtained

by non-linear least-squares fit according to Eq. (2). Subsequently, the K_i values were calculated using Eq. (3). The calculated K_i and n_H values are summarized in Table 2.

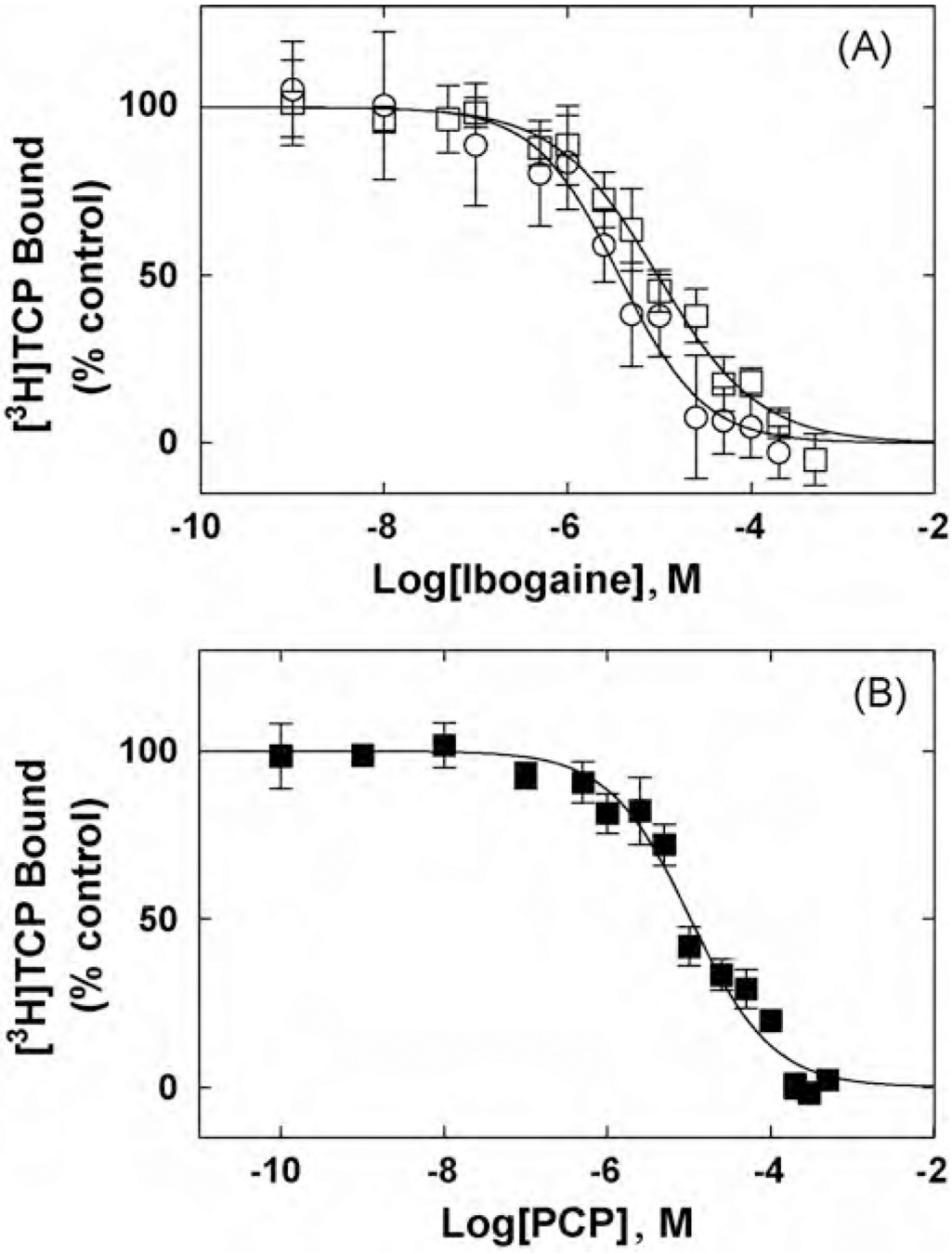

Fig. 4.

Inhibition of [^{3}H]TCP binding to ho3β4 AChRs in different conformational states elicited by (A) ibogaine and (B) PCP. hα3β4 AChR membranes (1.5mg/mL) were equilibrated (2 h) with 40 nM [^{3}H]TCP, in the absence (□,■) (AChRs are mainly in the resting state) or in the presence of 1 μM(−)-nicotine(○) (AChRs are mainly in the desensitized state), and increasing concentrations ofthe competitor. Nonspecific binding was determined at 100 μM ibogaine. From these plots the IC_{50} and n_H values were obtained by non-linear least-squares

fit according to Eq. (2). Subsequently, the K_i values were calculated using Eq. (3). The calculated K_i and n_H values are summarized in Table 2.

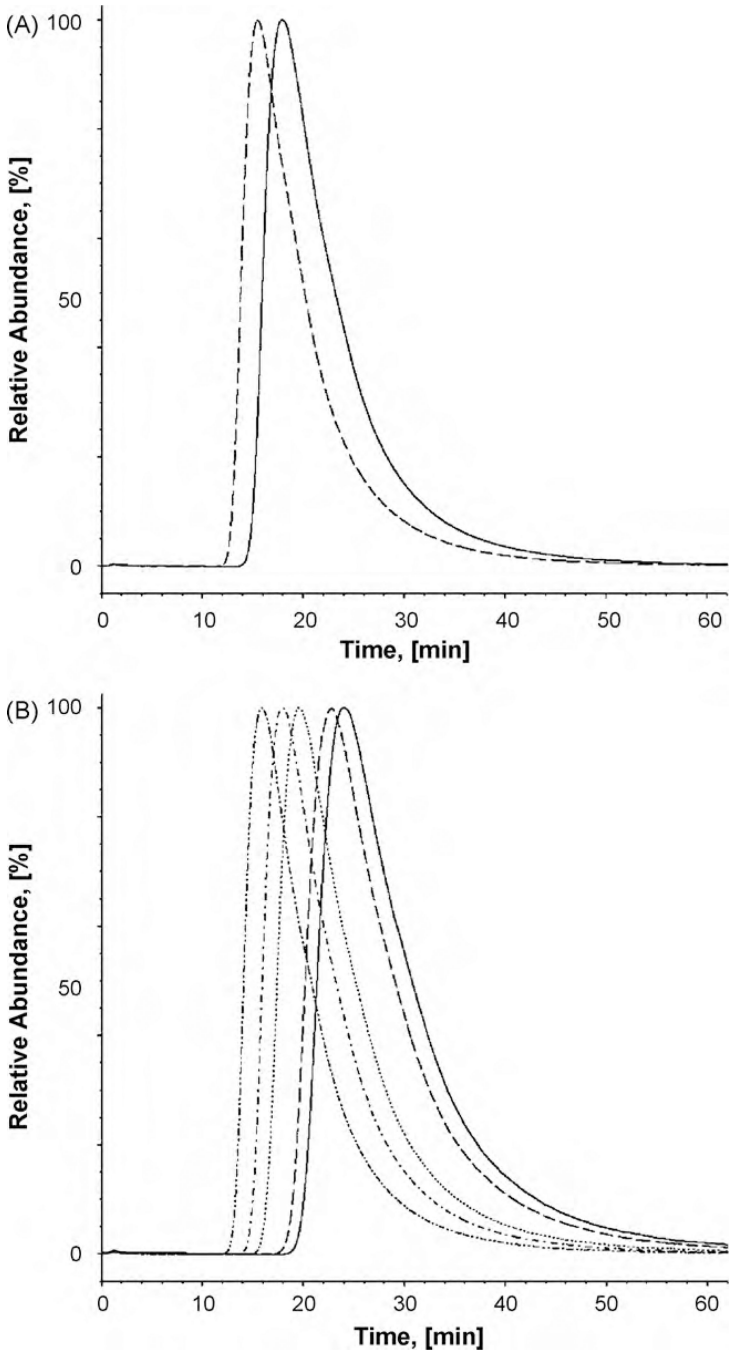

Fig. 5.

Chromatograhic elution of ibogaine from the CMAC-hα3β4 AChR column. (A) Ibogaine is eluted from the column with ammonium acetate buffer (10 mM, pH 7.4) and 15% methanol as the mobile phase, at 0.2mL/min and 20 °C. The dashed and straight lines represent the elution of ibogaine from the CMAC-hα3β4 AChR column in the presence of κ-BTx (the AChR is mainly in the resting state) and (±)-epibatidine (the AChR is mainly in the desensitized state), respectively. (B) Ibogaine is eluted from the CMAC-hα3β4 AChR

column in the presence of (±)-epibatidine (predominantly desensitized state) at different temperatures (from right to left: 10, 12,16, 20, and 25 °C).

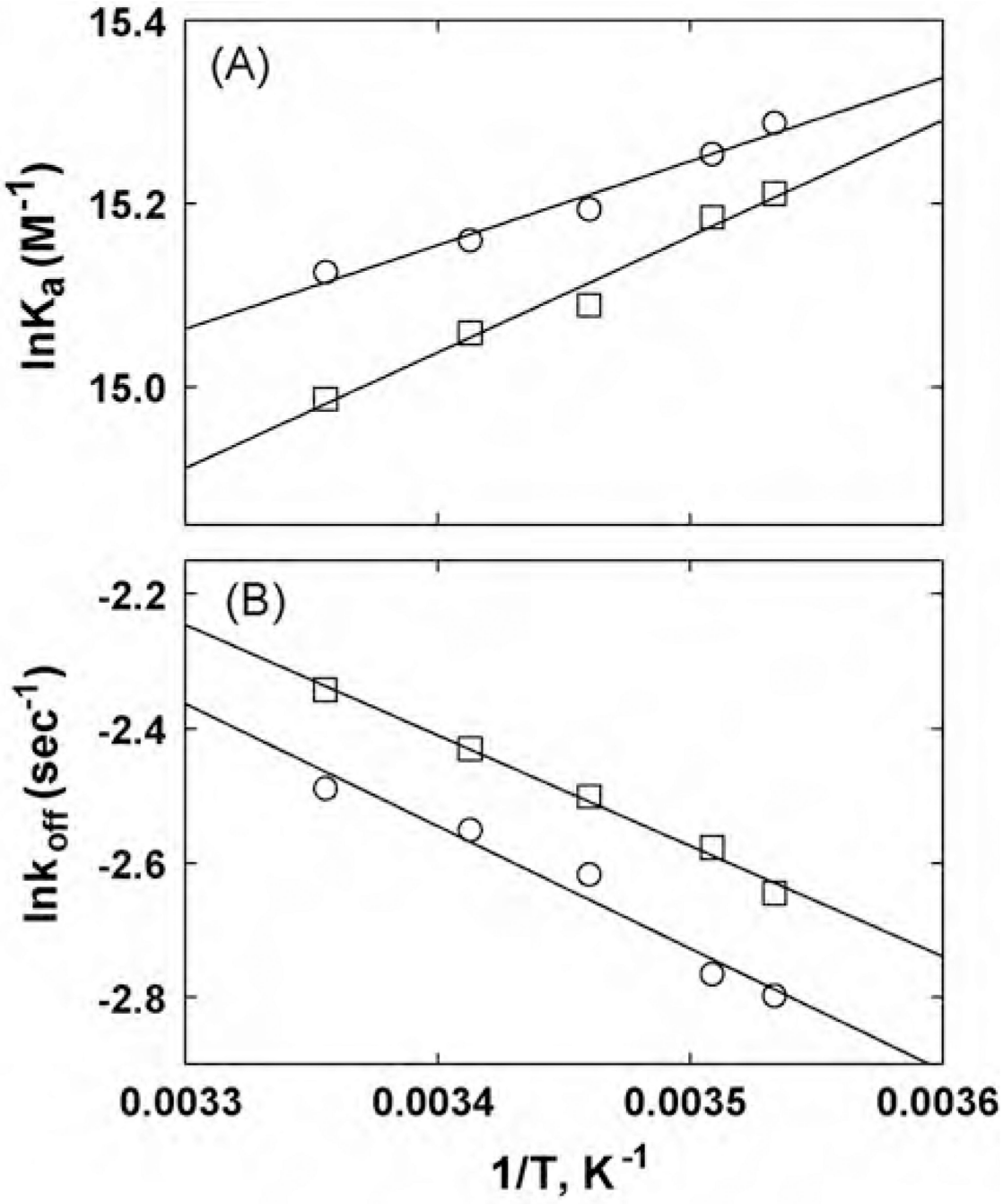

Fig. 6.

van't Hoff (A) and Arrhenius (B) plots for ibogaine determined by non-linear chromatography at different temperatures (see Fig. 5B). (A) van't Hoff plots were constructed by determining the K_a values of ibogaine at 10–25 °C, according to Eq. (5). The $\Delta H°$ and $\Delta S°$ values were calculated using the slope ($\Delta H°$ =−Slope R) and *y*-intersect ($\Delta S°$ = −*y*-intersect·*R*) values from the plots, according to Eq. (6), where *R* is the gas constant (8.3145 JK^{-1} mol^{-1}). (B) Arrhenius plots were constructed by determining the dissociation rate constants (k_{off}) of ibogaine at 10–25°C, according to Eq. (9). The E_a values were

calculated using the slope ($E_a = -\text{Slope}\cdot R$) from the plots, according to Eq. (10). Ibogaine was eluted from the column in the presence of (±)-epibatidine (○) (the AChR is mainly in the desensitized state) or κ-BTx (□) (the AChR is mainly in the resting state). The plots are the results from three experiments (n=3), where the S.D. error bars are smaller than the symbol size. The observed r^2 values for (A) are 0.977 (□) and 0.970 (○), and for (B) are 0.992 (□) and 0.960 (○), respectively, indicating that the plots are perfectly linear.

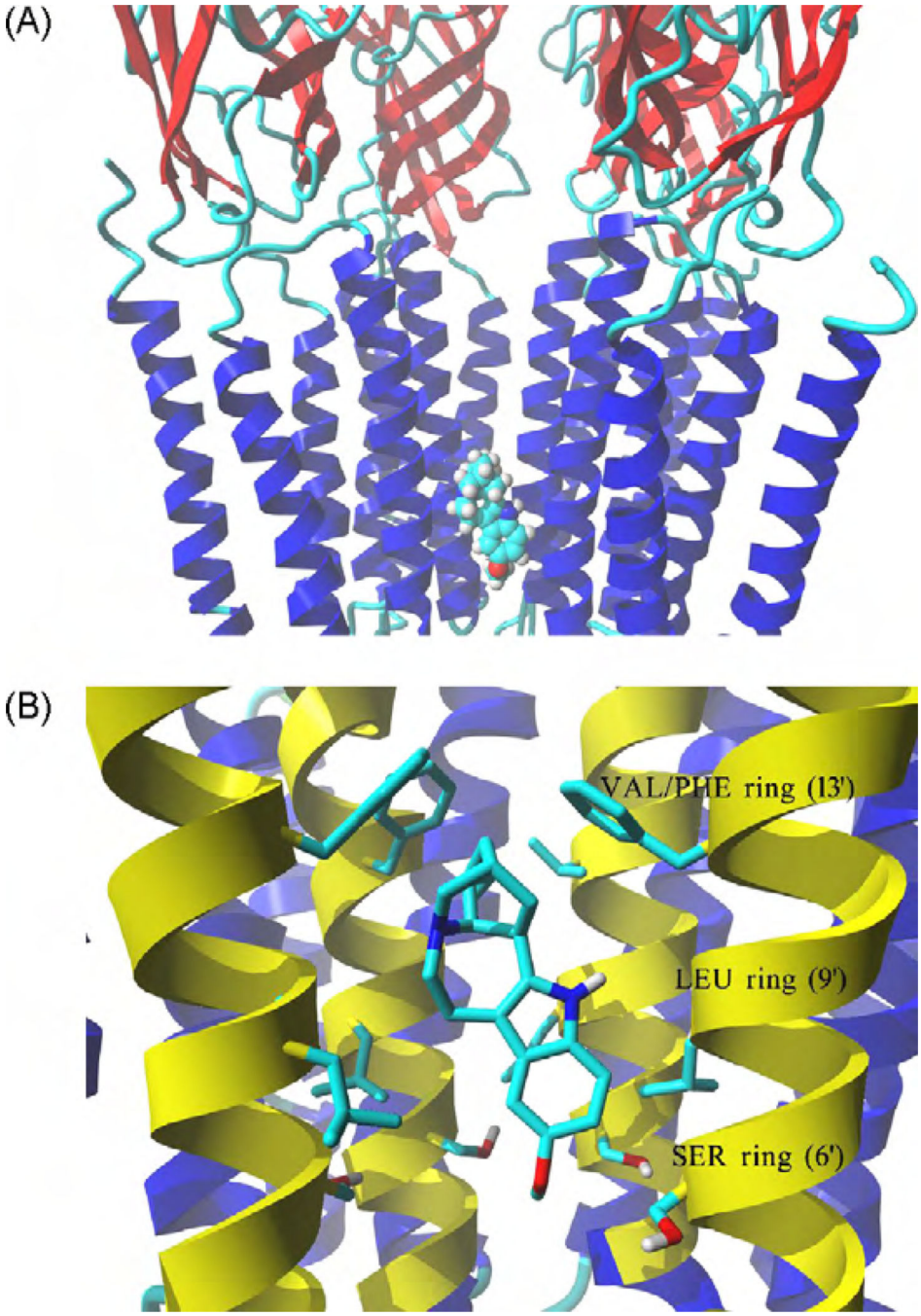

Fig. 7.

Model of the complex formed between ibogaine and the hα3β4 AChR ion channel. (A) Side view of the lowest energy pose for ibogaine showing four subunits rendered in secondary structure mode, whereas the ligand inthe neutral form is rendered in element color coded ball mode. Part of the receptor extracellular portion is also shown to have a better perspective of the ibogaine binding site location. (B) Interaction of the ibogaine molecule in the neutral state with the serine (SER) (position 6′), leucine (LEU) (position 9′), and valine/phenylalanine (VAL/PHE) (position 13′) rings. van der Waals interactions occur between

the aliphatic ring of ibogaine and the VAL/PHE (most important) and LEU rings, whereas its methoxy moiety forms hydrogen bonds with several hydroxyl groups at the SER ring. M2 transmembrane helices forming the wall of the channel are colored yellow, all othertransmembrane segments are blue. Residues from each ring are shown explicitly in stick mode. The ibogaine molecule is rendered in element color coded stick mode. All non-polar hydrogen atoms are hidden. For clarity, one α3 subunit is not shown explicitly, the order of the remaining subunits is from left to right: β4, β4, α3, and β4. (For interpretation of the references to color in this figure caption, the reader is referred to the web version of the article.)

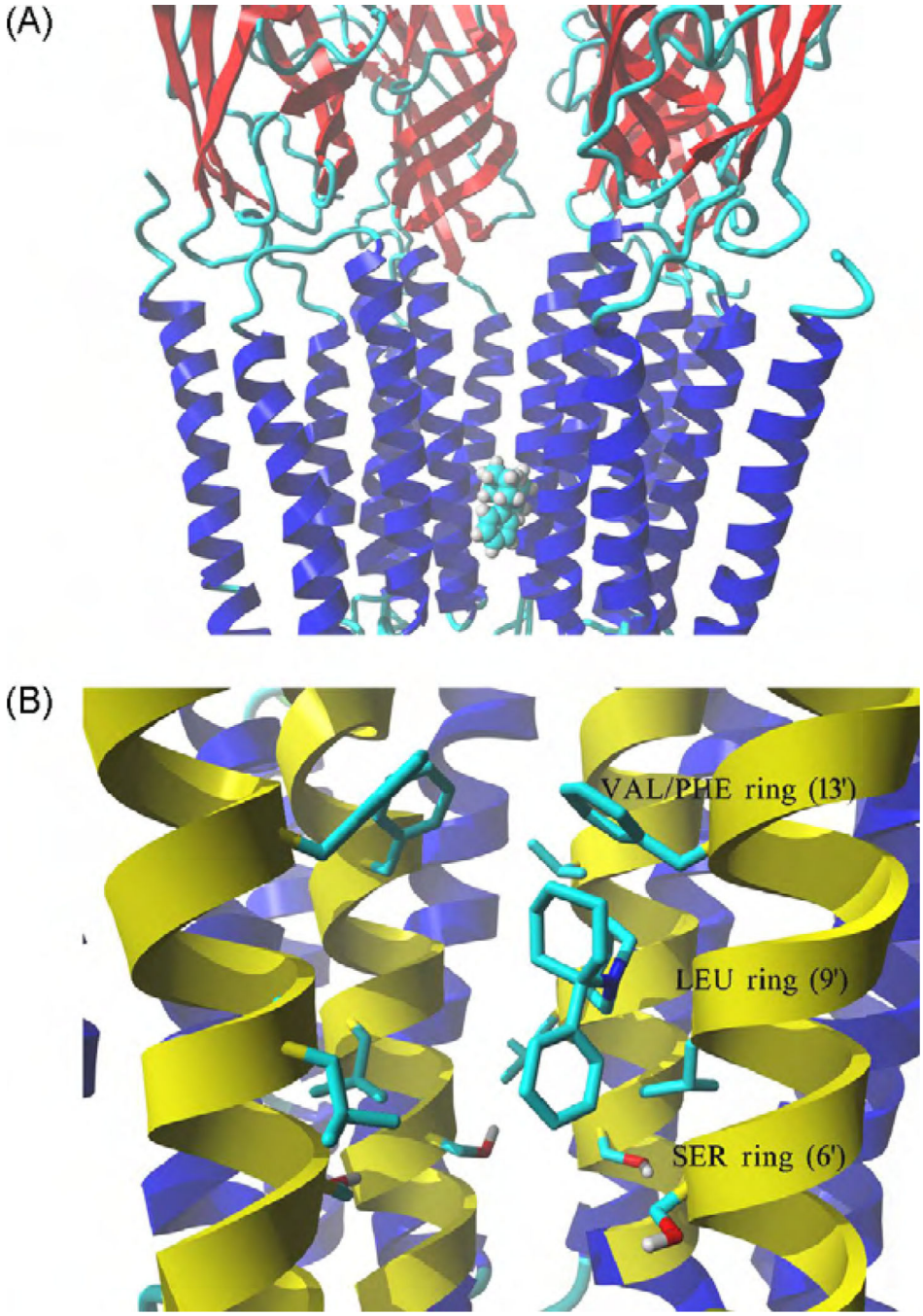

Fig. 8.

Model of the complex formed between PCP and the hα3β4 AChR ion channel. (A) Side view of the lowest energy pose for PCP showing four subunits rendered in secondary structure mode, whereas the ligand in the neutral form is rendered in element color coded ball mode. Part of the receptor extracellular portion is also shown to have a better perspective of the PCP binding site location. (B) Interaction of the PCP molecule in the neutral state with the serine (SER) (position 6′), leucine (LEU) (position 9’), and valine/phenylalanine (VAL/PHE) (position 13′) rings. van der Waals interactions occur between

the aliphatic ring of PCP and the VAL/PHE (most important) and LEU rings, and between the aromatic ring of PCP and the SER ring. M2 transmembrane helices forming the wall of the channel are colored yellow, all other transmembrane segments are blue. Residues from each ring are shown explicitly in stick mode. The PCP molecule is rendered in element color coded stick mode. All non-polar hydrogen atoms are hidden. For clarity, one α3 subunit is not shown explicitly, the order of the remaining subunits is from left to right: β4, β4, α3, and β4. (For interpretation of the references to color in this figure caption, the reader is referred to the web version of the article.)

Table 1

Inhibitory potency of ibogaine and PCP on hα3β4 AChRs determined by Ca^{2+} influx.

NCA	IC_{50} (μM)[a]	n_H[b]	Number of experiments (*n*)
Ibogaine	0.95 ± 0.13	1.24 ± 0.07	5
PCP	8.5 ± 1.4	0.92 ± 0.02	3

[a] The NCA concentration to produce 50% inhibition of (±)-epibatidine-induced Ca^{2+} influx was obtained from Fig. 1.

[b] Hill coefficient.

Table 2

Binding affinity of ibogaine and PCP for the hα3B4 AChR in different conformational states.

NCA	Radioligand	Resting		Desensitized	
		K_i (μM)	n_H	IC_{50} (μM)	n_H
Ibogaine	[^{3}H]Ibogaine	1.05 ± 0.12 *a*	0.82 ± 0.08	0.37±0.04 *c*	1.01 ±0.11
	[^{3}H]TCP	9.5 ± 1.9 *b*	0.79 ± 0.13	3.6±0.5 *d*	0.95 ±0.13
PCP	[^{3}H]Ibogaine	17 ± 2 *e*	0.88 ± 0.07	ND	ND
	[^{3}H]TCP	10 ± 2 *f*	0.87 ± 0.10	ND	ND

The ibogaine K_i values were obtained from Fig. 3A[a] and Fig. 4A[b], respectively, using Eq. (3), whereas the ibogaine IC_{50} values were obtained from Fig. 3A[c] and Fig. 4A[d], respectively, according to Eq. (2).

The PCP K_i values were obtained from Fig. 3B[e] and Fig. 4B[f], respectively, using Eq. (3).

n_H, Hill coefficient.

ND, not determined.

Table 3

Kinetic and thermodynamic parameters of ibogaine binding to hα3β4 AChRs in different conformational states determined by non-linear chromatography.

Parameter	AChR in the resting state[a]	AChR in the desensitized state[b]
k_{off} (s^{-1})	0.088 ± 0.001	0.078 ± 0.002
k_{on} (s^{-1} μM^{-1})	0.31 ± 0.02	0.30 ± 0.01
K_a (μM^{-1})	3.47 ± 0.12	3.84 ± 0.04
ΔG (kJ mol^{-1})	−36.7 ± 0.1	−36.9 ± 0.1

The chromatographic determinations using the CMAC-hα3β4 AChR column were performed in the presence of κ-BTx [a](the AChR is mainly in the resting state) or in the presence of (±)-epibatidine [b](the AChR is mainly in the desensitized state). The k_{off} and K_a values were empirically determined according to Eqs. (4) and (5), respectively, whereas the k_{on} values were calculated as $k_{on} = k_{off} \cdot K_a$.

The ΔG values were calculated using Eq. (6).

Table 4

Thermodynamic parameters of ibogaine binding to the hα3β4 AChR in different conformational states determined by non-linear chromatography.

Thermodynamic parameters	κ-BTx treated column[a]	Epibatidine treated column[b]
$\Delta H°$ (kJ mol^{-1})	−10.5 ± 0.7	−7.6 ± 0.3
$-T\Delta S°$ (kJmol-^{1})	−26.2 ± 0.7	−29.4 ± 0.3
ΔG^{20} (kJmol^{-1})	−36.7 ± 0.1	−37.0 ± 0.1
E_a (kJmol^{-1})	13.7 ± 0.7	15.1 ± 1.8
ΔH^+ (kJmol^{-1})	11.2 ± 0.7	12.7 ± 1.8

The elution of ibogaine from the CMAC-hα3β4 AChR column was performed in the presence of either κ-BTx [a](the AChR is mainly inthe resting state) or (±)-epibatidine [b](the AChR is mainly in the desensitized state).

The thermodynamic parameters $\Delta H°$ and $\Delta S°$ were calculated from Fig. 7A, according to Eq. (7), and the ΔG^{20} values were calculated using Eq. (8).

The E_a values for the process of drug dissociation were obtained from Fig. 7B, according to Eq. (9), and the ΔH^+ values were calculated using Eq. (10).